Strain Rate Dependent Poroelastic Behavior of Bovine Vertebral Trabecular Bone

Jung Hwa Hong, Mu Seong Mun
Korea Orthopedics and Rehabilitation Engineering Research Center, Inchon 403-120, Korea
Tae-Hong Lim
Biomechanics Laboratory, Department of Orthopaedic Surgery, Rush Presbyterian Medical College, IL 60611 U.S.A

It is widely accepted that the pressure variation of interstitial fluid is one of the most important factors in bone physiology. In order to understand the role of interstitial fluid on porous bony structure, a consideration for the biomechanical interactions between fluid and solid constituents within bone is required. In this study, a poroelastic theory was applied to investigate the elastic behavior of calf vertebral trabecular bone composed of the porous solid trabeculae and the viscous bone marrow. The poroelastic behavior of trabecular bone in a uniaxial stress condition was simulated using a commercial finite difference analysis software (FLAC, Itasca Consulting Group, USA), and tested for 5 different strain rates, i. e., 0.001, 0. 01, 0.1, and 10 per second. The material properties of the calf vertebral trabecular bone were utilized from the previous experimental study. Two asymptotic poroelastic responses, the drained and undrained deformations, were predicted. From the predicted results for the simulated five strain rates, it was found that the pore pressure generation has a linearly increasing behavior when the strain rate is the highest at 10 per second, otherwise it showed a nonlinear behavior. The pore pressure generation with respect to the strain was found to be increased as the strain rate increased. The elastic moduli predicted at each strain were 208.3, 212.2, 337.6, 593. 1, and 602.2 MPa, respectively. Based on the results of the present study, it was suggested that the calf vertebral trabecular bone could be modeled as a poroelastic material and its strain rate dependent material behavior could be predicted.

Key Words : Biomechanics, Trabecular Bone Mechanics, Theory of Poroelasticity, Strain Rate Effect, and Uniaxial Stress Condition

1. Introduction

Trabecular bone shows a porous structure composed of solid trabeculae and viscous intraosseous fluid. Trabecular bone occupies the proximal and distal parts of long bone and the inner most parts of spine, pelvis, and skull, to provide mechanical and physiological functions for mainly load bearing, impact energy absorption, and erthropoiesis. It shows high porosity (more than 85 %) compared to other biological hard tissues such as cortical bone having less than 10 % of porosity (Cowin, 1999). The pore space of trabecular bone is continuous to allow interstitial fluid flow (Hughes et al., 1978) and filled with a highly viscous biological fluid, mainly bone marrow which the viscosity is 67 times of water viscosity at 37 ℃ (Bryant, 1988). Therefore, trabecular bone can be defined as a highly porous structure filled with a highly viscous interstitial fluid. It is understood that observed time-dependent behavior of trabecular bone such as stress relaxation and creep (Ducheyne et al., 1977;

* Corresponding Author,
E-mail : msmun@iris.korec.re.kr
TEL : +82-32-500-0584 ; **FAX** : +82-32-512-9704
Korea Orthopedics and Rehabilitation Engineering Center, 47-3 Koosan-dong, Pupyong-ku Inchon 403-120, Korea.

Schoenfeld et al., 1974), influence of strain and loading rate input on mechanical properties (Carter and Hayes, 1977; Linde et al., 1991; Luo et al., 1993), and phase shift phenomena under dynamic loading (Tateishi, 1979), are caused by the interstitial bone fluid. To explain the time-dependent behavior of trabecular bone, therefore, mechanical roles of interstitial fluid occupying more than 85 % of the volume of trabecular bone should be included in analyses.

Since the late 1960's, the poroelasticity that accounts for coupled interaction between porous solid and viscous pore fluid has been used to investigate the time-dependent behavior of cortical bone. The creep and stress relaxation of cortical bone were predicted under a sudden application of load (Nowinski and Davis, 1969 and 1970; Nowinski, 1971 and 1972; Simon et al., 1985). The influence of the intraosseous boundary and loading conditions on the mechanical behavior of cortical bone were investigated at various loading conditions (Zhang and Cowin, 1994). The poroelasticity has been applied to understand the role of the intraosseous fluid in remodeling process of cortical bone (Arramon and Cowin, 1994; Harrigan and Hamilton, 1993; Johnson, 1982; Johnson et al., 1984; Weinbaum et al., 1994). These studies showed that the poroelasticity could be used to describe the time-dependent behavior of cortical bone. Recently, the application of poroelasticity to bone mechanics becomes important issue since the knowledge about the biomechanical interaction, particularly pore pressure generation, between the mineralized bone matrix and viscous intraosseous fluid is essential to understand the bone physiology concerning bone mineralization, osteocyte nutrition, and detailed bone remodeling process.

For trabecular bone, however, a few studies were performed using the theory of poroelasticity (Simon et al., 1985; Hong and Lim, 1998; Lim and Hong, 2000) although more significant time-dependent behaviors than cortical bone were observed in the previous experimental studies (Carter and Hayes, 1977; Ducheyne et al., 1977; Linde et al., 1991; Luo et al., 1993; Schoenfeld et al., 1974; Tateishi, 1979). A simple one-dimensional poroelastic modeling was performed and solved mathematically using assumed and estimated poroelastic properties to describe its time-dependent behavior (Hong and Lim, 1998). The results showed significant pore pressure effects by mechanical interaction between solid and fluid phases on the mechanical behavior of trabecular bone, although it was restrictive to the confined condition. The poroelastic properties based on the poroelastic formulations of Rice and Clearly (1976) were directly measured for the bovine vertebral trabecular bone (Lim and Hong, 2000). This study indicated that the pore pressure generation coefficient called Skempton's coefficient of trabecular bone is much higher than that of cortical bone (Lim and Hong, 2000; Cowin, 1999). Thus, the poroelastic effect of trabecular bone on its apparent mechanical behavior would be greater than that of cortical bone. However, no investigation is performed for the poroelastic behavior of trabecular bone using the experimentally measured poroelastic properties.

In this study, the porous elastic theory (Rice and Clearly, 1976) was applied to the bovine trabecular bone to investigate the effect of fluid phase on its apparent strain rate dependent behavior in an unconfined condition. For the study, the previously measured poroelastic properties of the bovine trabecular bone (Lim and Hong, 2000) were used. Since the theory covers elasticity of porous materials, the analysis was limited within the elastic range of the bovine trabecular bone. A possible viscoelastic effect of the trabecular matrix was neglected. The poroelastic behavior in a uniaxial stress condition was simulated by using an explicit finite difference analysis code for various strain rate inputs.

2. Porous Elastic Modeling in Uniaxial Stress Condition

A two-dimensional axisymmetric porous elastic model in the uniaxial stress condition was developed to investigate the pore pressure generation effect on enhancement of stiffness of the calf vertebral trabecular bone for various strain rates, 0.001, 0.01, 0.1, 1, and 10/sec. Figure 1 illustrates

the porous elastic model and boundary condition of a cylindrical trabecular bone sample (10 mm in diameter and 20 mm in length).

The stress-strain relationships in this configuration are (Rice and Clearly, 1976):

$$\sigma_{xx}=\alpha_1\varepsilon_{xx}+\alpha_2\varepsilon_{yy}+\frac{3(\nu_u-\nu)}{B(1+\nu)(1+\nu_u)}p$$
$$\sigma_{yy}=\alpha_1\varepsilon_{yy}+\alpha_2\varepsilon_{xx}+\frac{3(\nu_u-\nu)}{B(1+\nu)(1+\nu_u)}p \quad (1)$$
$$\sigma_{zz}=\alpha_2(\varepsilon_{xx}+\varepsilon_{yy})+\frac{3(\nu_u-\nu)}{B(1+\nu)(1+\nu_u)}p$$
$$\sigma_{xy}=\sigma_{yx}=2G\varepsilon_{xy}$$

where $\alpha_1=\frac{2G(1+\nu)}{3(1-2\nu)}+\frac{4}{3}G$ and

$\alpha_2=\frac{2G(1+\nu)}{3(1-2\nu)}-\frac{2}{3}G$.

The diffusion equation is:

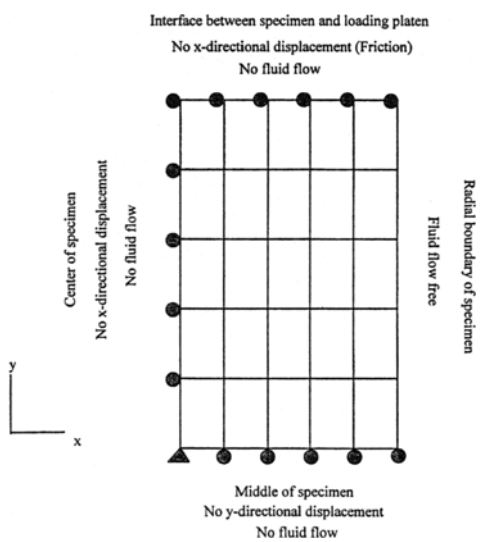

Fig. 1 Two-dimensional finite difference porous elastic model of the cylindrical trabecular bone specimen

$$\frac{\partial p}{\partial t}-\frac{2\kappa GB^2(1-2\nu)(1+\nu_u)^2}{9(\nu_u-\nu)(1-2\nu_u)}\left(\frac{\partial^2 p}{\partial x^2}+\frac{\partial^2 p}{\partial y^2}\right)=\frac{2GB(1+\nu_u)}{3(1-2\nu_u)}\frac{\partial}{\partial t}(\varepsilon_{xx}+\varepsilon_{yy}) \quad (2)$$

where G=shear modulus; ν=Poisson's ratio; ν_u=undrained Poisson's ratio; B=Skempton's coefficient; and κ=permeability coefficient. Initial and boundary conditions were: 1) no initial pore pressure and stress ($p(x, y, 0)=0$ and $\sigma_{xx}(x, y, 0)=\sigma_{yy}(x, y, 0)=\sigma_{zz}(x, y, 0)=\sigma_{xy}(x, y, 0)=0$); 2) pore pressure is always zero at the radial boundary ($p(D/2, y, t)=0$) where D is the diameter of the specimen; 3) due to symmetry, no longitudinal fluid flow at the middle ($y=0$) and at the end of the specimen ($y=L/2$), and no radial fluid flow at the center($x=0$), i. e., $\frac{\partial p(0, y, t)}{\partial x}=\frac{\partial p(x, 0, t)}{\partial y}=\frac{\partial p(0, L/2, t)}{\partial y}=0$ where L is the specimen length; 4) no longitudinal and radial displacement at the middle and center of the specimen, respectively, i. e., $\varepsilon_{xx}(0, y, t)=\varepsilon_{yy}(x, 0, t)=0$; and 5) due to friction between the specimen and loading platens, a radial fixed boundary condition is assumed $\varepsilon_{xx}(x, L/2, t)=0$). The detailed poroelastic formulations and meanings of parameters were described in the Appendix.

To obtain response, an explicit finite difference model was implemented using FLAC (Itasca Consulting Group, Minneapolis, MN, USA). The porous elastic parameters (Table 1) from literature (Lim and Hong, 2000) were used for the analysis. For the model predictions, the stress and pore pressure from each finite difference grid of the model were summed and then averaged at each time step. Since this study was limited within the elastic range of trabecular bone, an axial strain of 0.6 % (Keaveny et al., 1994) was applied to the analyses.

Table 1 Porous elastic parameters of the bovine vertebral trabecular bone used in this study (Lim and Hong, 1999)

Parameter	G	v	ν_u	B	κ
Value	90.85 (±59.59) MPa	0.242 (±0.099)	0.399 (±0.083)	0.851 (±0.144)	16.3 (±8.02) $\times 10^{-8}$ m^2/Pa.sec

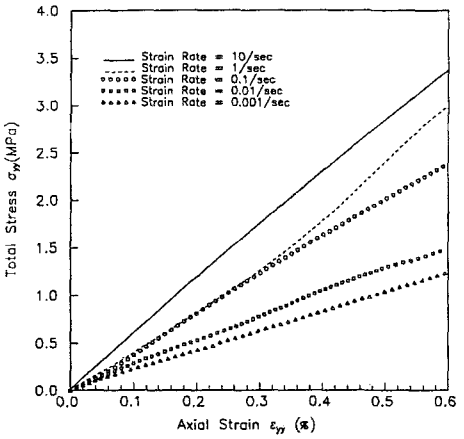

Fig. 2 Variation of the predicted total stress at five different strain rates using the poroelastic properties from the bovine vertebral trabecular bone

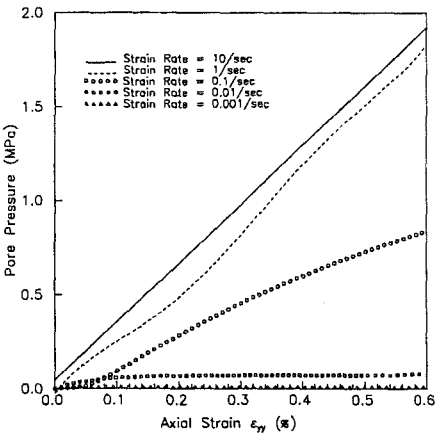

Fig. 3 Variation of the predicted pore pressure at five different strain rates using the poroelastic properties from the bovine vertebral trabecular bone

3. Results

The two-dimensional axisymmetric poroelastic problem was solved using a finite difference method to investigate the effect of coupled mechanical interactions between the fluid and solid phases of the bovine vertebral trabecular bone. Numerical solutions were obtained to investigate the effect of various strain rates (or loading speeds) of 0.001, 0.01, 0.1, 1, and 10 per second. The poroelastic properties of the bovine vertebral trabecular bone from the previous section used for model parameters to obtain the numerical solutions.

Figure 2 shows the total stress-strain curves predicted from the poroelastic model at 5 different strain rates in the uniaxial stress condition. For each strain rate, the total stress and pore pressure from the each finite difference grid of the model were summed and then averaged at each time step to simulate the load measured at load cell in the material testing machine. At the highest strain rate (10 per second), the predicted total stress-strain curve was nearly linear, implying that an undrained deformation occurred. A nearly linear total stress-strain curve was also predicted at the slowest strain rate, 0.001 per second, since the pore fluid flow was so slow and steady that negligible pore pressure was produced.

From the strain rate of 0.01 per second, the predicted total stress-strain curve became nonlinear, and more nonlinear at the strain rates of 0.1 and 1 per second. These changes in total stress-strain curves resulted from the changes in the pore pressure at various strain rates, as shown in Fig. 3 illustrating the changes in predicted pore pressure at various strain rates. For example, the pore pressure generation is almost negligible, and pore pressure has no effect on the total stress at the slowest strain rate (0.001 per second). However, pore pressure was substantially generated even at the slowest loading rate. At the strain rates of 0.01, 0.1, and 1 per second, the behavior of predicted pore pressure represent apparently nonlinear behavior. As a result, the nonlinear behavior of total stress was predicted.

4. Discussion

The strain rate effect on the mechanical properties of trabecular bone is frequently observed in the previous studies. The uniaxial stress condition is commonly used for measuring the mechanical properties of trabecular bone. Strain rate input has been most widely used for this purpose. While trabecular bone specimens with marrow *in situ* exhibits the influence of strain rate on mechanical properties under the uniaxial stress condition

(Han et al., 1996; Linde et al., 1991), no quantitative assessment has been made to understand the mechanism of changing mechanical properties at various strain rate inputs. Particularly, the effect of intraosseous fluid pressure on the mechanical properties of trabecular bone in an uniaxial condition has never been investigated although it is generally believed that the enhancement of mechanical properties may be caused by the intraosseous fluid (Carter and Hayes, 1977; Ducheyne et al., 1977). The two-dimensional axisymmetric poroelastic model was developed in this study to investigate the effect of pore fluid and strain rate on the mechanical behavior of bovine vertebral trabecular bone in the elastic range. This investigation is the first analytical study using the measured poroelastic properties of trabecular bone to analyze its poroelastic behavior.

As noted in the poroelastic constitutive Eq. (1), a total stress resulting from a strain input can vary due to the pore pressure generation that can be estimated by solving the diffusion Eq. (2). The amount of pore pressure generated within the representative element of volume is affected by several factors, such as the poroelastic properties, the volumetric deformation rate, and boundary conditions. For example, a maximum pore pressure would be generated regardless of the other factors when the pore fluid is trapped in the porous solid because of the confined boundary condition. This called an undrained deformation. Such an asymptotic deformation also would be possible at least for a short time period even in a free fluid flow boundary condition during a very fast deformation since the pore fluid has no time to move within the representative element of volume. On the other hand, pore pressure generation is negligible in a drained condition. When a poroelastic material in an unconfined boundary condition undergoes static (or quasi-static) loading, there is a sufficient time for the pore pressure to equilibrate to the boundary pressure. Assuming zero boundary pressure, a negligible pore pressure is generated within the entire representative element of volume during deformation.

These two asymptotic poroelastic responses were well predicted from the poroelastic model of bovine vertebral trabecular bone (Fig. 2 and 3). The pore pressure generation was greatest and increased linearly at the fastest strain rate (10 per second), while the pore pressure generation was smallest and maintained minimum value during the deformation at the slowest strain rate (0.001 per second). The difference in pore pressure generation resulted in a significant increase in the predicted total stress at the fastest strain rate.

In intermediate conditions between the undrained and drained conditions, the permeability coefficient was shown to mainly affect the pore pressure generation in poroelastic materials (Hong and Lim, 1998). Since the permeability coefficient represents a resistance of interstitial fluid flow, its magnitude governs the pore pressure diffusion incorporated with other four-poroelastic properties. When poroelastic materials undergo an intermediate loading between the very fast and quasi-static in the uniaxial stress condition, the volumetric deformation rate is not sufficiently fast or slow to form an undrained or drained condition. Dissipation and generation of pore pressure occur while interstitial fluid flows within a poroelastic material and across its boundary. A difference between the generated and dissipated pore pressures determines a total stress variation and thus an apparent stiffening behavior of poroelastic materials. Incorporating the poroelastic properties into the pore pressure diffusion phenomena, the pore pressure was predicted to change nonlinearly (Fig. 3), and the total stress showed a nonlinear increase (Fig. 2) in the intermediate strain rates (0.01, 0.1, and 1 per second).

The compressibility of the fluid and solid phases may significantly affect the pore pressure generation and thus the deformation of poroelastic materials. The compressibility of a material is defined as an inverse of bulk modulus. The bulk modulus (or modulus of compression) is the ratio of the compressive stress to the cubical compression, i. e., the hydrostatic pressure state. The bulk modulus can be defined by an elastic relationship: $K=E/\{3(1-2\nu)\}$ where K is the bulk modulus; E is the elastic modulus; and ν is the Poisson's

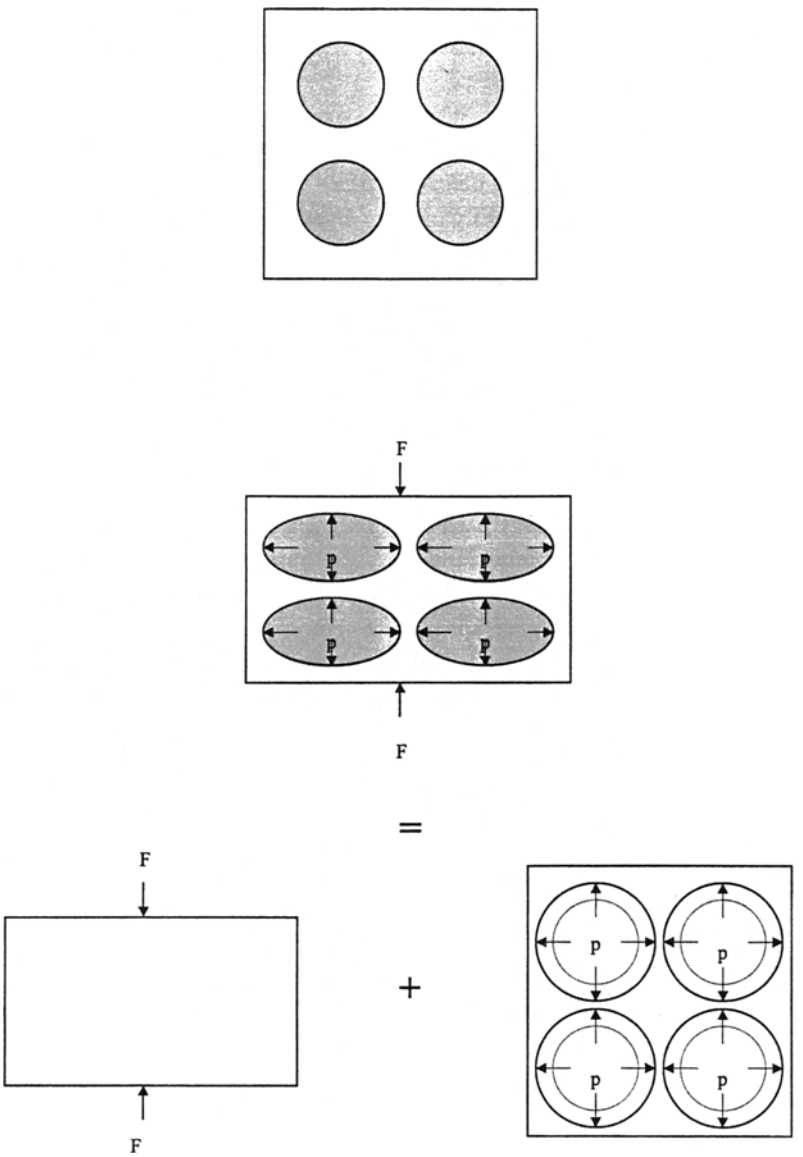

Fig. 4 Deformation of an idealized microstructure of poroelastic material

ratio. When the Poisson's ratio varies from -1 to 0.5 in an isotropic elastic range, the bulk modulus changes $E/9$ to ∞. Thus, a hydraulic pressure tends to diminish the bulk volume for all physical materials. An isotropic material is incompressible only when the Poisson's ratio is 0.5. Since the pore pressure in a poroelastic material is hydrostatic, the solid matrix should experience the hydraulic pressure during deformations. The effect of compressibility of solid and fluid constituents of poroelastic material is considered as a major factor to alter its poroelastic behavior at the continuum level (Detournay and Cheng, 1993; Green and Wang, 1986). For example, Fig. 4 illustrates the deformation of solid matrix in an undrained condition schematically when a porous material saturated with fluid undergoes a volumetric deformation. The effect of compressibility on the deformation of a poroelastic material can be decomposed into two states. An application of external force on the poroelastic material composed of compressible constituents causes

a bulk deformation of solid skeleton (state 1). The bulk deformation generates a pore pressure in pores of the material. The resulting pore pressure induces a dilation of pores (state 2). The bulk deformation and dilation of pores of the poroelastic material result in the combined deformation (state 1+state 2). The compressibility of solid and fluid phases affects the bulk deformation of solid skeleton and dilation of pores. This interaction between the fluid and solid phases affects the deformation of a poroelastic material until the deformation terminates. For example, there is negligible pore pressure and thus no dilation of pore space for a poroelastic material filled with highly compressible fluid constituent. Thus, the material behaves like a porous elastic material without fluid. For the incompressible constituents model, the bulk deformation of solid skeleton represents the reduction of pore space without any dilation of pores.

The poroelastic model developed in this study has some limitations. First of all, the model was developed based on the assumption of uniform pore distribution in the representative element of volume. An irregular pore distribution would result in changes in the elastic properties as well as localized permeability changes. This would be able to be incorporated by using different poroelastic properties in each element in the model. Secondly, the isotropic properties trabecular bone was assumed for the model development. In case of anisotropy, the estimation of the drained shear modulus values from the relationship among the elastic modulus, drained shear modulus, and drained Poisson's ratio would not be valid. Furthermore, the permeability coefficient value used in this study was along the cephalad-caudal direction, while the fluid flow in the model would occur in the lateral as well as axial directions. Thus, the anisotropic property of trabecular bone would result in different model behavior. More sophisticated study is recommended considering the anisotropic poroelastic properties of trabecular bone in the future.

References

Arramon, Y. P. and Cowin, S. C., 1994, "Strain Rate as a Bone Remodeling Stimulus," *ASME, BED-28*, pp. 259~260.

Bryant, J. D., 1988, "On the Mechanical Function of Marrow in Long Bone," *Proc. Instn. Mech. Engrs., Part H, J. Eng. Med.*, Vol. 17, pp. 55~58.

Carter, D. R. and Hayes, W. C., 1977, "The Compressive Behavior of Bone as a Two-Phase Porous Structure," *J. Bone Jt. Surg.*, Vol. 59A, pp. 954~962.

Cowin, S. C., 1999, "Bone Poroelasticity," *J. Biomech.*, Vol. 32, pp. 217~238.

Detournay, E. and Cheng, H. D., 1993, *Fundamentals of Poroelasticity. Comprehensive Rock Engineering: Principles, Practice and Projects (Hudson, J. edited)*, Vol. 2, pp. 113~171, Pergamon Press.

Ducheyne, P., Heymans, L., Martens, M., Aernoudt, E., de Meester, P. and Mulier, J. C., 1977, "The Mechanical Behavior of Intracondylar Cancellous Bone of the Femur at Different Loading Rates," *J. Biomech.*, Vol. 10, pp. 747~762.

Green, D. H. and Wang, H. F., 1986, "Fluid Pressure Response to Undrained Compression in Saturated Sedimentary Rock," *Geophys.*, Vol. 51, pp. 948~956.

Han, S., Medige, J., Faran, K., Feng, Z., and Ziv, I., 1996, "Effect of Loading Rate on the Prediction of Mechanical Properties of Trabecular Bone by Ultrasonic Velocity and Attenuation," *Trans. Orthop. Res. Soc.*, Vol. 21, p. 82.

Harrigan, T. P. and Hamilton, J. J., 1993, "Bone Strain via Transmembrane Potential Changes in Surface Osteoblasts: Loading Rate and Microstructural Implications," *J. Biomech.*, Vol. 26, pp. 183~200.

Hong, J. H. and Lim, T. H., 1998, "Poroelastic Model of Trabecular Bone in Uniaxial Strain Condition," J. Musculoskeletal Res., Vol. 2, pp. 167~180.

Huges, M. S., Davies, R., Khan, R., and Kelly, P., 1978, "Fluid Space in Bone," *Clin. Orthop.*

Res., Vol. 134, pp. 332~341.

Johnson, M. W., 1984, "Behavior of Fluid in Stressed Bone and Cellular Stimulation," *Calcif. Tissue Int.*, Vol. 36 (S), pp. 72~76.

Johnson, M. W., Chakkalakal, D. A., Harper, R. A., Karz, J. L., and Rouhana, S. W., 1982, "Fluid Flow in Bone," *J. Biomech.*, Vol. 11, pp. 881~885.

Keaveny, T. M., Guo, X. E., Wachtel, E. F., McMahon T. A., and Hayes, W. C., 1994, "Trabecular Bone Exhibits Fully Linear Elastic Behavior and Yields at Low Strains," *J. Biomech.*, Vol. 27, pp. 1127~1136.

Lim, T. H. and Hong, J. H., 2000, "Poroelastic Properties of Bovine Vertebral Trabecular Bone," J. Orthop. Res., Vol. 18, pp. 671~677.

Linde, F., N∅rgaard, P., Hvid, I., Odgaard, A., and S∅balle, K., 1991, "Mechanical Properties of Trabecular Bone. Dependence on Strain Rate," *J. Biomech.*, Vol. 24, pp. 803~809.

Luo, Z. P., Ochoa, J. A., and Hillberry, B. M., 1993, "Effects of Specimen Size on Hydraulic Stiffening of Cancellous Bone," *Trans. Orthop. Res. Soc.*, Vol. 18, p. 174.

Nowinski, J. L. and Davis, F. C., 1969, "The Flexure and Torsion of Bones as Anisotropic Poroelastic Materials," *In proceeding 7th Ann. Meet. Soc. Eng. Sci.*

Nowinski, J. L. and Davis, F. C., 1970, "The Human Skull as a Poroelastic Spherical Shell Subjected to a Quasi-Static Load," *Mathem. Biosci.*, Vol. 8, pp. 397~416.

Nowinski, J. L., 1971, "Bone Articulations as Systems of Poroelastic Bodies in Contact," *J. Amer. Inst. Aeron. Astron.*, Vol. 9, pp. 62~67.

Nowinski, J. L., 1972, "Stress Concentration Around a Cylindrical Cavity in a Bone Treated as a Poroelastic Body," *Acta Mechanica*, Vol 13, pp. 281~192.

Rice, J. R. and Cleary, M. P., 1976, "Some Basic Stress-Diffusion Solutions for Fluid Saturated Elastic Porous Media with Compressible Constituents," *Res. Geophys. Space Phys.*, Vol. 14, pp. 227~241.

Scheidegger, A. E., 1957, *The Physics of Flow Through Porous Media*, University of Toronto Press.

Schoenfeld, C. M., Lautenschlager, E. P., and Meyer, P. R., 1974, "Mechanical Properties of Human Cancellous Bone in Femoral Head," *Med. Biol. Eng.*, Vol. 12, pp. 313~317.

Simon, B. R., Wu, J. S. S., Carlton, M. W., Kazarian, L. E., France, E. P., Evans, J. H., and Zienkiewicz, O. C., 1985, "Poroelastic Dynamic Structural Models of Rhesus Spinal Motion Segments," *Spine*, Vol. 10, pp. 494~507.

Tateishi, T., 1979, "Rheological Characteristics of Human Joints," *Recent Research on Mechanical Behavior Solids*, pp. 179~204, Univ. Tokyo Press, Tokyo, Japan.

Weinbaum, S., Cowin, S. C. and Zeng, Y., 1994, "Excitation of Osteocytes by Mechanical Loading Induced Bone Fluid Shear Stress," *J. Biomech.*, Vol. 27, pp. 339~360.

Zhang, D. and Cowin, S. C., 1994, "Oscillatory Bending of a Poroelastic Beam," *J. Mech. Phys. Solids*, Vol. 42, pp. 1575~1599.

Appendix

A.1 Theory of Poroelasticity

Stress exerted on a control volume element of a fluid-filled porous material (total stress) produces both strains and changes in pore pressure in the control element. Rice and Cleary (1976) reformulated the relationship among the total stress, strain, and pore pressure using unique material parameters (Table A). Assuming the

Table A. Porous elastic parameters based on Rice and Clearly's formulation

Parameters	
G	Shear Modulus
v	Poisson's Ratio
v_u	Undrained Poisson's Ratio
B	Skempton's Pore Pressure Build-up Coefficient
κ	Permeability Coefficient

isotropy of the porous elastic material, the constitutive equations were defined as:

$$\sigma_{ij}+\frac{3p(\nu_u-\nu)}{B(1-2\nu)(1+\nu_u)}\delta_{ij}=2G\varepsilon_{ij}+\frac{2G\nu}{1-2\nu}\varepsilon_{kk}\delta_{ij} \quad (A1)$$

where σ_{ij}=total stress tensor (MPa); ε_{ij}=strain tensor; p=pore pressure (MPa); δ_{ij}=Kronecker delta (if $i=j$, then $\delta_{ij}=1$, if $i\neq j$ then $\delta_{ij}=0$); and i, $j=1$, 2, 3 (the summation convention applies when repeated indices are used).

The diffusion equation that governs pore pressure generation with volumetric deformation of the control element is Detournay and Cheng, (1993):

$$\frac{\partial p}{\partial t}-\frac{2\kappa GB^2(1-2\nu)(1+\nu_u)^2}{9(\nu_u-\nu)(1-2\nu_u)}\nabla^2 p=-\frac{2GB(1+\nu_u)}{3(1-2\nu_u)}\frac{\partial \varepsilon_{kk}}{\partial t} \quad (A2)$$

where t=time; $\nabla^2\equiv\sum_{i=1}^{3}\frac{\partial^2}{\partial x_i^2}$(the Laplacian operator); and ε_{kk}=the trace of strain tensor or volumetric strain.

When a porous elastic material deforms without generating a pore pressure (p=0.0), Eq. (A1) becomes the constitutive equation for an isotropic elastic solid material:

$$\sigma_{ij}=2G\varepsilon_{ij}+\frac{2G\nu}{1-2\nu}\varepsilon_{kk}\delta_{ij} \quad (A3)$$

where G=shear modulus and ν=Poisson's ratio. Such a deformation with zero pore pressure generation can occur when a quasi-static load is applied to porous elastic material in a drained condition in which the interstitial fluid can flow across the boundary with no resistance. Thus, this was called a drained deformation, and G and ν were named as the shear modulus and the Poisson's ratio, respectively.

The other asymptotic behavior of a porous elastic material is called an undrained deformation since it occurs in an undrained condition in which the interstitial fluid is totally prevented from flowing out of the control volume element across the boundary. During the undrained deformation, a porous elastic material can be treated as an elastic material with the same shear modulus (G) but different Poisson's ratio, i. e., the undrained Poisson's ratio (ν_u). The corresponding constitutive equations can be expressed as (Detournay and Cheng, 1993):

$$\sigma_{ij}=2G\varepsilon_{ij}+\frac{2G\nu_u}{1-2\nu_u}\varepsilon_{kk}\delta_{ij} \quad (A4)$$

The theoretical range of ν_u is $\nu\leq\nu_u\leq 0.5$.

Skempton's pore pressure build-up coefficient (B) was defined as the ratio of the pore pressure increment (Δp) to the mean stress increment ($\Delta\sigma_{kk}/3$) during an undrained deformation (Green and Wang, 1986) $B=-3\Delta p/\Delta\sigma_{kk}$. Thus, B indicates the load bearing capability of the fluid constituent that is caused by the restricted fluid flow across the boundary. In general, B varies from 0.0 to 1.0 (Rice and Clearly, 1976).

The relationship between B and ν_u is $\alpha B=[3(\nu_u-\nu)]/[(1-2\nu)(1+\nu_u)]$, where α is the Biot coefficient of effective stress and ν is the Poisson's ratio. B and ν_u are known to be related with the compressibility of both solid and fluid constituents. Their values represent the porous elastic effects such as the sensitivity of the volumetric response to the rate of loading and the rate of pore pressure generation. For example, B and ν_u values are 1.0 and 0.5, respectively, for a porous elastic material consisting of the incompressible solid and fluid constituents in which the porous elastic effects are strongest. When the fluid constituent becomes more compressible, some of the porous elastic effects disappear, and B and ν_u become closer to 0.0 and ν, respectively.

The permeability coefficient (κ) is a well known parameter which describes how the interstitial fluid can flow through the pores in a porous elastic material. k is known to be sensitive to the viscosity of the fluid as well as to the geometrical factors, such as pore size and tortuosity (Scheidegger, 1957).